Advances in Military Technology
Vol. 20, No. 2, 2025, pp. 361-373
ISSN 1802-2308, eISSN 2533-4123
DOI 10.3849/aimt.01977

Research on Coil Design to Improve Performance of Disc-Shaped Magnetorheological Brakes

N. Anh Ngoc, N. Minh Duc, N. Minh Tien, and H. Quang Tuan*

School of Mechanical and Automotive Engineering, Hanoi University of Industry, Vietnam

The manuscript was received on 4 March 2025 and was accepted after revision for publication as an original research paper on 30 June 2025.

Abstract:

This study investigates the impact of various coil parameters on the working efficiency of disc-form magnetorheological brakes (MRBs). While earlier research predominantly addressed coil shape and count, the present work examines less-explored factors, including coil installation position and conductor diameter. Finite Element Method (FEM) simulations were performed to analyze the relationships among braking torque, coil geometry, and applied current, with a particular focus on enhancing the torque-to-mass ratio (T/M) to optimize both performance and cost-effectiveness. Results demonstrate that reducing the air gap between the coil and the MR fluid layer effectively concentrates magnetic flux, yielding a substantial increase in braking torque. The study offers comprehensive insights into coil design and configuration and proposes recommendations to improve MRB performance while maintaining economic feasibility.

Keywords:

Magnetorheological Brake (MRB), coil design, Torque-to-Mass Ratio (T/M), Finite Element Method (FEM)

1 Introduction

Magnetorheological Brakes (MRBs) have garnered significant attention in recent years due to their flexible braking capabilities and energy efficiency. Among MRB configurations, the disc brake type stands out with its compact design and superior braking performance [1-5]. A crucial factor influencing the performance of MRBs is the magnetorheological fluid (MR fluid). This fluid has the ability to alter its viscosity when exposed to a magnetic field, thereby adjusting the braking force when current is applied to the coil, allowing for precise control of braking force. Recent advancements in MR fluid technology, including the integration of nanoparticles, have enhanced its

* *Corresponding author: School of Mechanical and Automotive Engineering, Hanoi University of Industry, 298 Cau Dien Street, Bac Tu Liem District, Hanoi, Vietnam. Phone: +84 09 88 59 88 60, E-mail: tuanhq@haui.edu.vn*

rheological responsiveness, improved thermal stability, and increased oxidation resistance, thereby ensuring stable braking performance over extended periods [6-8].

Furthermore, improving the properties of magnetorheological fluids, including reducing frictional losses and enhancing magnetization capabilities, continues to be the focus of numerous studies [9-11]. Another important area is optimizing the disc brake structure. Research has highlighted the advantages of multi-layered disc brake designs, which increase the contact area with the magnetic flux and improve braking torque [12]. The use of advanced materials, such as composites and alloys with high magnetic permeability, has enhanced the durability and magnetic performance of these materials [13]. Temperature management during operation also plays a crucial role in maintaining the reliability and efficiency of MRBs. Excessive temperatures during operation can degrade both the MR fluid and the coil. Proposed solutions include liquid cooling systems and advanced heat dissipation mechanisms to ensure stable performance under high-load conditions or prolonged use[14].

In recent years, there have been numerous efforts to investigate the impact of coil configuration on MRB performance. Sohn et al. [15] conducted experimental studies on the effect of coil shape on braking torque and demonstrated that a new coil design generates approximately 10 % greater torque compared to traditional MR brakes when operating within a current range of 0.5 A to 2.0 A, with a maximum torque of 4.1 Nm at 2.0 A. Similarly, Nguyen et al. [16] studied the effect of the number of coils on power consumption and weight, finding that brakes with single coil, double coil, and triple coil had weights of 1.56 kg, 1.34 kg, and 1.28 kg, respectively, while the corresponding power consumption was 29.8 W, 36.5 W, and 49.5 W. Nguyen et al. [17] also confirmed these findings by comparing traditional MRB and optimized MRB, reporting stable braking torques of 9.7 Nm and 9.75 Nm, respectively.

Despite these advancements, current studies primarily focus on coil shape and number, while neglecting other important parameters such as coil positioning and installation method. This study will address these gaps by systematically investigating different coil positions and conductor sizes, aiming to identify optimal configurations that maximize braking torque while maintaining a high torque-to-mass ratio (T/M). Using finite element simulations, this study aims to propose a comprehensive design framework to enhance MRB performance.

2 Methodology

2.1 Mathematical Model for Determining Braking Torque

Studies often employ the Bingham model [18] when investigating the rheological behavior of magnetorheological fluid (MRF) due to the simplicity of the model and its minimal experimental data requirements. The resulting shear stress is then determined as follows:

$$\tau = \tau_{\mathrm{y}} + \mu \frac{r\Omega}{d} = \tau_{\mathrm{y}} + \mu \frac{\Omega\left(R_{\mathrm{i}} + l\sin\varphi\right)}{d} \tag{1}$$

where τ_{y} is the yield stress in the field-free state; μ is the viscosity of the MRF; Ω is the magnitude of the angular velocity of the rotor; d is the gap size of the MRF flow.

The differential equation of the MRF torque is based on the study [18] shown in Fig. 1.

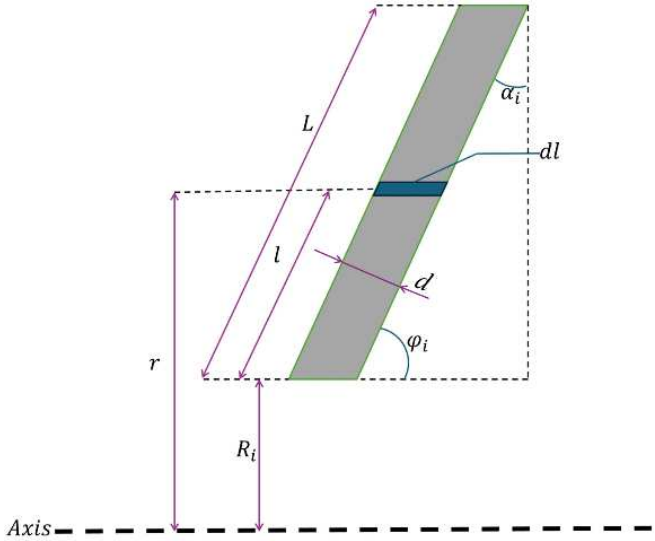

Fig. 1 Closed circular element of MR fluid in the oil gap

$$\mathrm{d}T = r\tau \mathrm{d}A = 2\pi r^2 \tau \mathrm{d}l = 2\pi\left(R_\mathrm{i} + l\sin\varphi_\mathrm{i}\right)^2 \tau \mathrm{d}l \tag{2}$$

where r is the radius of the MRF element relative to the MRB's axis of rotation; R_i is the lower radius of the oil gap relative to the axis of rotation; $\varphi_\mathrm{i} = 90° - \alpha_\mathrm{i}$ is the angle between the oil gap and the axis of rotation; l is the length of the oil gap; A is the area subjected to stress; α_i is the inclination angle of the disc; L is the expected length of the oil gap relative to the axis of rotation.

From Eqs (1) and (2), we obtain the formula for calculating the torque in each region.

$$T_\mathrm{i}\left(i = E_\mathrm{i}, C\right)$$

$$T_\mathrm{i} = 2\pi\int_0^\mathrm{L}\left(R_\mathrm{i} + L\sin\varphi_\mathrm{i}\right)^2 \tau dl = 2\pi\int_0^\mathrm{L}\left(R_\mathrm{i} + L\sin\varphi_\mathrm{i}\right)^2\left[\tau_\mathrm{y} + \mu\frac{\Omega\left(R_\mathrm{i} + l\sin\varphi_\mathrm{i}\right)}{\mathrm{d}}\right]\mathrm{d}l \tag{3}$$

The braking torque of each oil region is then calculated as follows:

$$\left.\begin{aligned} T_\mathrm{i} = {} & 2\pi\left(R_\mathrm{i}^2 L + R_\mathrm{i} L^2\sin\varphi_\mathrm{i} + \frac{1}{3}L^3\sin^2\varphi_\mathrm{i}\right)\tau_y + \\ & + \frac{1}{2}\pi\mu\frac{L\Omega}{d_\mathrm{i}}\left(4R_\mathrm{i}^3 + 6R_\mathrm{i}^2 L\sin\varphi_\mathrm{i} + 4R_\mathrm{i} L^2\sin^2\varphi_\mathrm{i} + L^3\sin^3\varphi_\mathrm{i}\right) \end{aligned}\right\} \tag{4}$$

Assuming the neglect of the torque generated by the sealing and load-bearing components in the MR brake, the torque T_MRB generated on both surfaces of the brake disc with flat surfaces is illustrated in Fig. 2.

$$T_\mathrm{MRB} = 2\left(T_\mathrm{E1} + T_\mathrm{E2} + T_\mathrm{E3} + T_\mathrm{E4} + T_\mathrm{E5} + T_\mathrm{E6} + T_\mathrm{E7} + T_\mathrm{E8} + T_\mathrm{E9} + T_\mathrm{E10} + T_\mathrm{E11}\right) + T_\mathrm{C} \tag{5}$$

$T_{\mathrm{E}j}$ is the torque of the oil regions on the brake disc surface (j = 1 to 11),
T_C is the torque of the oil region on the top surface of the brake disc.

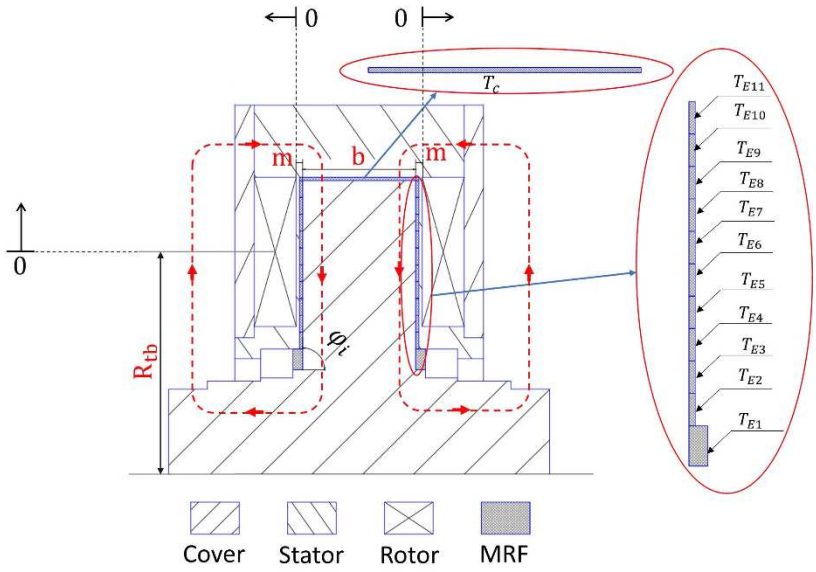

Fig. 2 Magnetorheological fluid region of the MRB device

The yield stress (τ_γ) is based on experimental results published by Lord Corporation in Fig. 3.

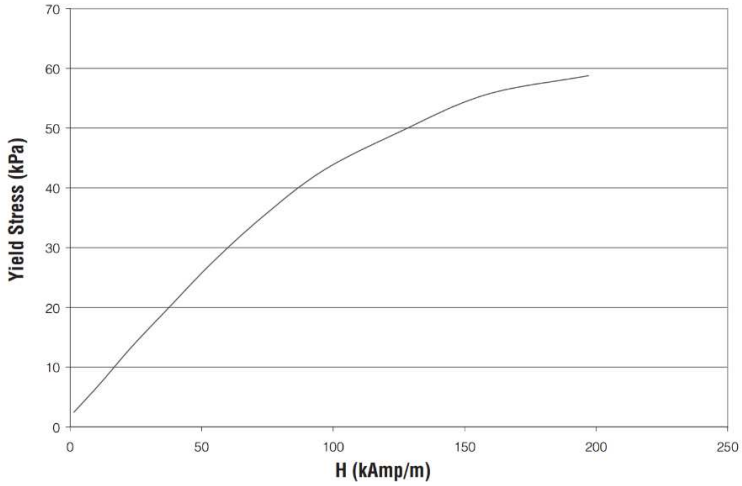

Fig. 3 Characteristic curve of MRF-140CG magnetorheological fluid [19]

By using Curve-fitting method with a 6th-degree polynomial, the relationship between shear stress and the magnetic field strength of the MRF-140CG oil grade is determined as follows:

$$\tau_y = k_0 + k_1 H_{MRF}^1 + k_2 H_{MRF}^2 + k_3 H_{MRF}^3 + k_4 H_{MRF}^4 + k_5 H_{MRF}^5 + k_6 H_{MRF}^6 \quad (6)$$

where H_{MRF} is the magnetic field intensity; k_i is the coefficient of the Curve-fitting equation in Tab. 1

Tab. 1 Coefficients of the Curve-fitting equation for MRF-140CG [19]

k_0	k_1	k_2	k_3	k_4	k_5	k_6
1.7318	0.4726	9.83×10^{-4}	-1.75×10^{-5}	-2.78×10^{-8}	7.13×10^{-10}	-1.8×10^{-12}

2.2 Ampère's Law of Magnetic Field and the Applied Current Intensity to the Coil

The magnetic flux density B generated when applying current I to the coil is determined by Ampère's law as follows:

$$B = \mu_0 \mu_r \frac{NI}{L_c} \tag{7}$$

where B is the magnetic flux density (tesla, T); μ_r is the relative permeability of the magnetic core (with air, H, μ_r = 1); μ_0 is the magnetic permeability of vacuum ($4\pi \times 10^{-7}$ H/m); N is the number of coils; I is the current through the coil [A]; L_c is the length of the coil [m].

2.3 Method for Determining the Braking Mass of MRB

The total mass of the brake is calculated based on the combined mass of the main components, including the rotor, stator, and coil. In the calculation, the mass of certain auxiliary parts (such as bearings and seals) is neglected for simplicity. The total mass M is expressed as follows:

$$\begin{aligned} M &= M_{\text{Coil}} + M_{\text{Rotor}} + M_{\text{Stator}} + M_{\text{MRF}} \\ M &= V_{\text{Coil}}\rho_{\text{Coil}} + V_{\text{Rotor}}\rho_{\text{Rotor}} + V_{\text{Stator}}\rho_{\text{Stator}} + V_{\text{MRF}}\rho_{\text{MRF}} \end{aligned} \tag{8}$$

where V and ρ are the volume and density of each material, respectively. According to the technical data [19-21]: $\rho_{\text{Coil}} = 8.933 \times 10^{-6}$ kg/mm^3, $\rho_{\text{Rotor}} = 7.87 \times 10^{-6}$ kg/mm^3, $\rho_{\text{MRF}} = 3.64 \times 10^{-6}$ kg/mm^3, V_{Rotor}, V_{Stator} calculated based on the model input into the software and $V_{\text{Coil}} = \pi\left(\frac{d}{2}\right)^2 L_c$.

When the distance m from the coil to the MRF oil layer or the average radius R_{tb} of the coil changes, the distribution and impact of the magnetorheological fluid (MRF) layer will change significantly. This change directly affects the braking torque generated by the disc brake. Additionally, adjusting the coil parameters not only impacts the braking characteristics but also affects the layout, installation, and overall structure of the braking system. Therefore, the study of the working efficiency of the magnetorheological disc brake should be based on evaluating not only the braking torque generated by the MRB but also the torque-to-mass (T/M) ratio of the device. This approach aims to ensure a comprehensive assessment of both performance and suitability in the design.

2.4 Magnetic Field Simulation of MRB Braking

Mesh Generation of the Model

The investigated cases are performed using the Finite Element Method (FEM) based on Altair's Flux software. The mesh used is a regular tetrahedral mesh, consisting of four triangular faces. Tetrahedral meshing is well-suited for efficiently filling complex computational domains that contain regions requiring both coarse and fine mesh densi-

ties. In addition, this mesh type optimizes computational time compared to other element types while maintaining high convergence during simulation processes [22]. For this meshing model, it is crucial to carefully select the mesh size to ensure the accuracy of magnetic field interactions between different surfaces. The optimal mesh size depends on the desired level of detail. To accelerate the meshing process, a value closer to 0 should be used, whereas a value closer to 1 indicates a coarser mesh. In this specific case, an average mesh size of 0.5 mm was applied [23] (Fig. 4 and Tab. 2).

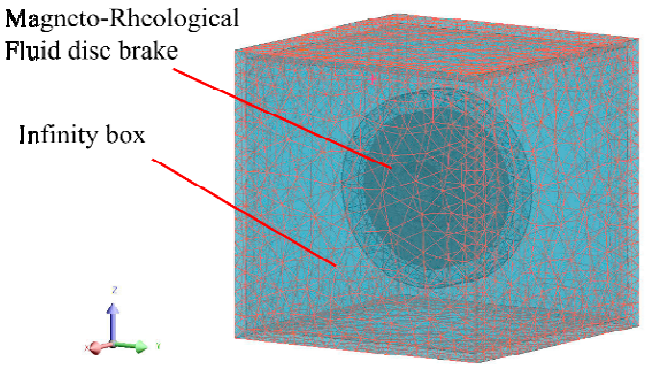

Fig. 4 Mesh model of the surrounding environment

Tab. 2 Meshing parameter

Elements not evaluated	0 %
Excellent quality elements	60.24 %
Good quality elements	26.89 %
Average quality elements	4.97 %
Poor quality elements	7.9 %
Number of nodes	178 205
Number of surface elements	209 286
Number of volume elements	1 037 159

Materials

In this study, steel 1010XC10 is a commonly used soft magnetic material with high magnetic permeability, low magnetic reluctance, and low resistivity, as illustrated by the magnetic induction curve in Fig 5., and with a mass density of 7 870 kg/m^3 [20]. This type of steel helps enhance the magnetic field strength for the MRF layer of the brake. It will be used to simulate the components: rotor and stator.

For this study, MRF-140CG was chosen for investigation, which is a product developed by Lord Corporation. This fluid is responsible for transmitting force and generating the magnetic friction effect in magnetorheological brakes, characterized by high yield stress, low viscosity, and the ability to operate in high-temperature conditions. These properties are listed in Tab. 3.

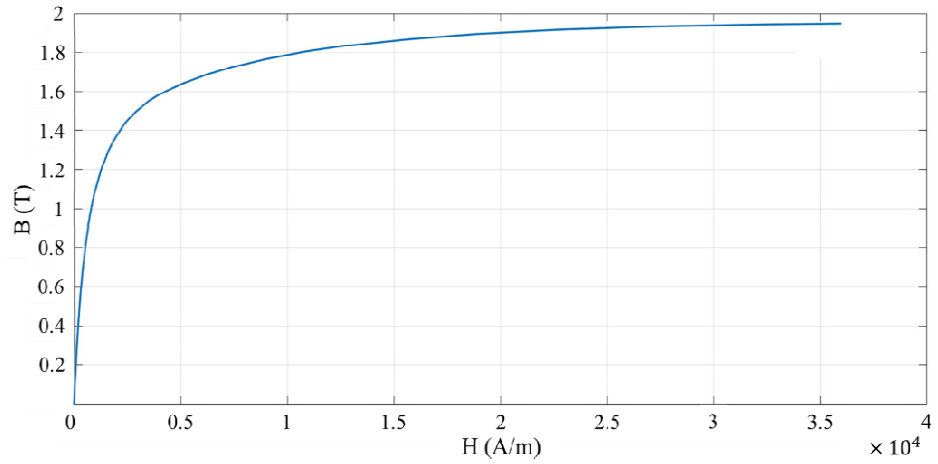

Fig. 5 B-H Curve of Steel 1010XC10

Tab. 3 Properties of Magnetorheological Fluid MRF-140CG [19]

Carrying particle	Density [g/cm^3]	Viscosity [Pa s]	Operating temperature [°C]	Fluid content [%]	Flash point [°C]
Hydrocarbon	3.54-3.74	0.280 ± 0.070	(−40)-130	85.44	>150

Boundary Conditions

In Flux software, three typical magnetic field problems are supported in a 3D model: static magnetic field, dynamic magnetic field, and steady-state magnetic field. However, for this study, the problem selected for simulation is the static magnetic field, where materials are considered at a fixed current. The steady-state magnetic field is considered with a controlled current over a range. Due to the magnetorheological fluid's phase transition from liquid to semi-solid, the software is unable to meet the calculation requirements. The magnetic field analysis will be carried out in the static magnetic field environment with different current change intervals.

In this study, the conditions for solving the problem are established by varying the current values. Specifically, the current used ranges from 0 A to 3 A, with a step change of 0.25 A. This demonstrates the relationship between the generated torque and current intensity during braking. For the configurations under investigation, two coils are symmetrically placed on either side of the stator. To enhance the magnetic field strength, the two coils will be supplied with opposite currents. This condition ensures that the magnetic field remains stable. The angular velocity of the rotating shaft is maintained at a constant value of Ω = 15.26 rad/s. The temperature is assumed to be constant, and the effects of temperature on the magnetic properties and viscosity of the magnetorheological fluid are neglected. Additionally, the model must ensure axial symmetry and consistency in the physical properties of the materials. The magnetorheological fluid is assumed to be homogeneous, without stratification, sedimentation, or turbulent flow.

3 Results and Discussion

3.1 Effect of Coil Distance (m) on Braking Torque (T_{MRB}) with Varying Current Intensity (I)

Fig. 6 shows the braking torque of the MRB as the current intensity varies from 0 A to 3 A, with the coil distance to the magnetorheological fluid layer (m) ranging from 0 mm to 15 mm. The angular velocity of the brake disc is examined at a low-speed range of Ω = 15.26 rad/s, with an oil gap of d = 1 mm, and the MRF grade used is 140CG. Upon detailed observation, it can be seen that as the distance m increases from 0 mm to 15 mm, the braking torque (T_{MRB}) gradually decreases, regardless of the current intensity (I). Furthermore, the highest braking torque is recorded when m = 0 mm, as the magnetic field is more concentrated near the fluid layer. Simultaneously, when m > 10 mm, the braking efficiency significantly decreases, indicating that a large distance weakens the magnetic field considerably. This is entirely consistent with the physical theory of magnetic fields and current. Specifically, the stronger the current, the stronger the magnetic field generated ($B \sim I$). However, if the distance is too large, a strong magnetic field cannot compensate for the loss caused by the dispersion of the magnetic flux.

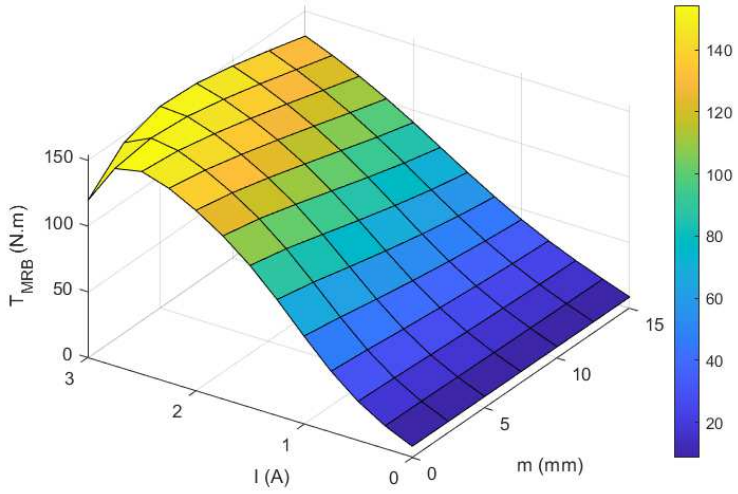

Fig. 6 Relationship between the braking torque generated by MRB as the coil distance to the oil layer changes at different current intensities

Specifically, at m = 0 mm, increasing I to 3 A results in the greatest increase in braking torque (up to 140 Nm). As m increases to 15 mm, increasing I is no longer effective, with the braking torque only reaching below 50 Nm. This is because the dispersion of the magnetic flux becomes more dominant as m increases, significantly reducing the magnetic field strength at the magnetorheological fluid layer. Additionally, the interaction between current and distance is nonlinear due to other factors such as e.g. the magnetic saturation effect of the core material. Based on the survey results, the study suggests maintaining the distance $m \leq 5$ mm to ensure a sufficiently strong magnetic field at the MR fluid layer to enhance the MRB's braking torque.

3.2 Change in the Average Radius of the Coil (Rtb)

The results of the braking torque generated when changing the average radius of the coil (R_{tb}) are shown in Fig. 7. The coil parameters used in the simulation are taken from Tab. 4:

Tab. 4 Change in the average radius of the coil

Coil radius	Wire diameter	Coil height	Coil width	Wire length	Number of coil	Fill factor
R_{tb}	D [mm]	H [mm]	W [mm]	L_c [m]	N [–]	f_f [%]
69.25	0.5	13	46.5	1 167.4	2 683	87.15
70.25				1 167.4	2 645	85.91
71.25				1 167.4	2 608	84.70
72.25				1 167.4	2 572	83.53
73.25				1 167.4	2 536	82.39
74.25				1 167.4	2 502	81.28
75.25				1 167.4	2 469	80.20
76.25				1 167.4	2 437	79.15
77.25				1 167.4	2 405	78.12
78.25				1 167.4	2 374	77.12
79.25				1 167.4	2 344	76.15
80.25				1 167.4	2 315	75.20
81.25				1 167.4	2 287	74.28
82.25				1 167.4	2 259	73.37
83.25				1 167.4	2 232	72.49
84.25				1 167.4	2 205	71.63

Key observations from the 3D plot (Fig. 7a) indicate that the braking torque (T_{MRB}) increases as the current intensity (I) increases. At fixed values of R_{tb}, as I increases, the braking torque increases consistently. At I = 3 A, the braking torque reaches its highest value, exceeding 200 Nm. Furthermore, the effect of the average radius (R_{tb}) on the braking torque can be observed. The braking torque T_{MRB} gradually increases as R increases from 65 mm to about 72 mm. When R_{tb} exceeds 72 mm, the braking torque tends to decrease slightly or stabilize, depending on the current intensity (I). The highest braking torque is achieved at $R_{tb} \approx 72$ mm and I = 3.0 A.

Fig. 7b shows the variation range of the braking torque with R_{tb}. As R_{tb} changes from 65 mm to 85 mm, the braking torque T_{MRB} changes significantly. At a current of I = 3.0 A, the braking torque peaks at R_{tb} = 72 mm (around 180 Nm) and decreases as R_{tb} increases further. At lower current levels ($I \leq 2.0$ A), the braking torque does not

change much with R_{tb}. In contrast, at higher current levels (I > 2.5 A), changes in R_{tb} have a significant impact on braking torque. This can be explained by the fact that when R_{tb} increases from 65 mm to around 72 mm, the magnetic field effectiveness increases as the coil reaches a higher efficiency region of the magnetic core. When R_{tb} exceeds 72 mm, the magnetic field slightly weakens due to the dispersion of the magnetic flux at the core's edge. Moreover, braking torque is linearly dependent on current ($B \sim I$), so at higher current levels, the stronger magnetic field increases braking force. However, at lower current levels, the effect of increasing R_{tb} on braking torque is limited.

Based on the survey results, the study proposes a coil design with $R_{tb} \approx 72$ mm as the optimal value for achieving the highest braking torque. It is recommended to avoid designs with R_{tb} greater than 75 mm, as braking efficiency decreases and it leads to wasted space and materials.

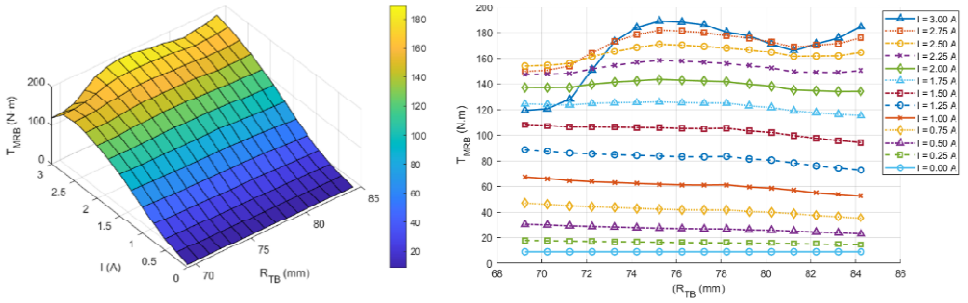

a) b)

Fig. 7 a) Relationship between the braking torque generated by MRB as the current intensity changes at different average coil radii; b) Relationship between the braking torque generated by MRB as the average coil radius changes at different current intensities.

Additionally, increasing the average coil radius means raising the coil placement cavity in the stator, which directly affects the overall mass of the brake. Therefore, the choice of an appropriate configuration depends not only on the torque generated but also on the torque-to-mass (T/M) ratio.

Fig. 8 shows the T/M ratio as two variables, current intensity and average coil radius, change.

The results indicate that as R_{tb} increases from 65 mm to around 72 mm, the T/M ratio increases significantly, showing the highest coil mass efficiency in this region. When R_{tb} exceeds 72 mm, the T/M ratio gradually decreases due to the mass increase outweighing the contribution of braking torque. The T/M ratio increases sharply as I increases from 1.0 A to 3.0 A, reaching its optimal value at the highest current level (I = 3.0 A). At lower current levels ($I \leq 1.5$ A), the T/M efficiency is low and varies little with R_{tb}. This is because, when the coil radius increases from 65 mm to around 72 mm, the effective magnetic field region increases, helping to increase braking torque without significantly raising the mass. In the case of R_{tb} exceeding 72 mm, the coil mass increases faster than the improvement in the magnetic field, resulting in a reduction in the T/M ratio. At higher current levels, the generated magnetic field is stronger, improving the torque generation efficiency, which significantly increases the T/M value. The T/M ratio reaches its maximum at R_{tb} = 72 mm and I = 3.0 A, with the best mass efficiency. The T/M ratio decreases when R_{tb} exceeds 72 mm due to the

imbalance between mass and the generated braking torque. Based on this, the study suggests selecting an average radius of $R_{tb} \approx 72$ mm, where the largest T/M ratio is achieved. It is important to avoid increasing R_{tb} beyond 75 mm to minimize unnecessary mass increase.

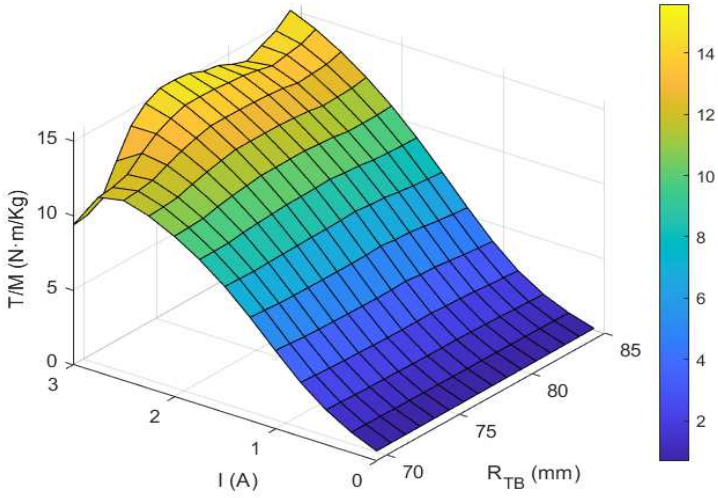

Fig. 8 Relationship between the T/M ratio as the average coil radius changes at current levels from 0 A to 3 A

4 Conclusion

This study analyzed the impact of coil parameters, such as position, average radius, wire diameter, and magnetic field distribution, on the braking performance of the magnetorheological brake (MRB) in disc form. Through finite element simulations and curve fitting techniques, the study provided valuable insights into the relationship between braking torque, the torque-to-mass ratio (T/M), and coil design. Key findings indicate that reducing the gap between the coil and the magnetorheological fluid layer enhances magnetic flux concentration, significantly increasing braking torque. Furthermore, the optimal average radius for the coil was determined to be approximately 72 mm, which maximizes the T/M ratio while maintaining an effective magnetic flux density. The study highlights the importance of optimizing coil design parameters to achieve a reasonable balance between braking performance and system mass. The recommendations presented in this study provide a practical foundation for improving the efficiency and cost-effectiveness of MRB systems, particularly in applications that demand high performance and low weight. In the future, experimental validation of the proposed models and the exploration of advanced materials will be crucial to further enhance the performance of MRBs.

References

[1] ASSADSANGABI, B., F. DANESHMAND, N. VAHDATI, M. EGHTESAD and Y. BAZARGAN-LARI. Optimization and Design of Disk-Type MR Brakes. *In-*

ternational Journal of Automotive Technology, 2011, **12**(6)**,** pp. 921-932. DOI 10.1007/s12239-011-0105-x.

[2] KARAKOC, K. *Design of a Magnetorheological Brake System Based on Magnetic Circuit Optimization* [online]. 2007 [viewed 2025-05-05]. Available from: https://dspace.library.uvic.ca/server/api/core/bitstreams/1d9d831c-5486-4712-b294-fda034f5634f/content

[3] TUAN, H.Q. and T.M. HOANG. Simulation-Based Investigation of the Effects of Major Rameters on Magnetorheological Brake Torque. *Journal of Southwest Jiaotong University,* 2023, **58**(3), pp. 244-251. ISSN 0258-2724.

[4] SHAMIEH, H. and R. SEDAGHATI. Design Optimization of a Magneto-Rheological Fluid Brake for Vehicle Applications. In: *Proceedings of the ASME 2016 Conference on Smart Materials, Adaptive Structures and Intelligent Systems. Volume 2: Modeling, Simulation and Control; Bio-Inspired Smart Materials and Systems; Energy Harvesting*. Stowe: American Society of Mechanical Engineers, 2016. DOI 10.1115/SMASIS2016-9084.

[5] QUANG, T.H., H.T. MINH, N.N. ANH and T.T. THANH. Determination of Magnetorheological Brake Characteristics by Experiment on the Test Rig. In: *Proceedings of the 3rd Annual International Conference on Material, Machines and Methods for Sustainable Development (MMMS2022)*. Cham: Springer, 2022, pp. 395-401. DOI 10.1007/978-3-031-31824-5_47.

[6] SPAGGIARI, A. and E. DRAGONI. Effect of Pressure on the Flow Properties of Magnetorheological Fluids. *Journal of Fluids Engineering*, 2012, **134**(9), 091103. DOI 10.1115/1.4007257.

[7] WANG, H.Y., H.Q. ZHENG, Y.X. LI and S. LU. Mechanical Properties of Magnetorheological Fluids Under Squeeze-Shear Mode. In: *Fourth International Symposium on Precision Mechanical Measurements*. Anhui: SPIE, 2008, pp. 607-612. DOI 10.1117/12.819634.

[8] ZIMMERMAN, D.T., R.C. BELL, J.A. FILER, J.A. KARLI and N.M. WERELEY. Elastic Percolation Transition in Nanowire-Based Magnetorheological Fluids. *Applied Physics Letters,* 2009, **95**(1), 014102. DOI 10.1063/1.3167815.

[9] QUOC, N.V., L.D. TUAN, L.D. HIEP, H.N. QUOC and S.B. CHOI. Material Characterization of MR Fluid on Performance of MRF Based Brake. *Frontiers in Materials,* 2019, **6,** 125. DOI 10.3389/fmats.2019.00125.

[10] SHAH, K. and S.B. CHOI. The Influence of Particle Size on the Rheological Properties of Plate-Like Iron Particle Based Magnetorheological Fluids. *Smart Materials and Structures,* 2014, **24**(1), 015004. DOI 10.1088/0964-1726/24/1/015004.

[11] SINGH, R.K. and C. SARKAR. Characterization of Magnetorheological Brake in Shear Mode Using High-Strength MWCNTs and Fumed Silica-Based Magnetorheological Fluids at Low Magnetic Fields. *Journal of Tribology,* 2023, **145**(3), 031702. DOI 10.1115/1.4056042.

[12] POKAAD, A.Z. and A.Z. ZAINORDIN. Magnetorheological Braking Torque Prediction Using Multiple Disk Arrangements. In: *AIP Conference Proceedings*. Melville: AIP Publishing, 2024, 020021. DOI 10.1063/5.0240150.

[13] KADAM, S., A.K. KARIGANAUR and H. KUMAR. Torque Generation in Lightweight Four Rotor Magnetorheological Brake. *Sādhanā,* 2024*,* **49**, 261. DOI 10.1007/s12046-024-02607-8.

[14] TUAN, H.Q., V.H. QUAN and T.M. HOANG. Thermal Analysis of the MRB During Downhill Braking. *International Journal of Mechanical Engineering and Robotics Research,* 2025*,* **14**(3), pp. 245-251. DOI 10.18178/ijmerr.

[15] SOHN, J.W., H.G. GANG and S.B. CHOI. An Experimental Study on Torque Characteristics of Magnetorheological Brake with Modified Magnetic Core Shape. *Advances in Mechanical Engineering,* 2018*,* **10**(1), 1687814017752222. DOI 10.1177/1687814017752222.

[16] NGUYEN, N.D., T.T. NGUYEN, D.H. LE and Q.H. NGUYEN. Design and Investigation of a Novel Magnetorheological Brake with Coils Directly Placed on Side Housings Using a Separating Thin Wall. *Journal of Intelligent Material Systems and Structures,* 2021*,* **32**(14), pp. 1565-1579. DOI 10.1177/1045389X21993912.

[17] NGUYEN, Q.H., N.D. NGUYEN and S.B. CHOI. Design and Evaluation of a Novel Magnetorheological Brake with Coils Placed on the Side Housings. *Smart Materials and Structures*, 2015, **24**(4), 047001. DOI 10.1088/0964-1726/24/4/047001.

[18] LI, W.H. and H. DU. Design and Experimental Evaluation of a Magnetorheological Brake. *The International Journal of Advanced Manufacturing Technology,* 2003*,* **21**, pp. 508-515. DOI 10.1007/s001700300060.

[19] *MRF-140CG Magneto-Rheological Fluid – 1 Liter* [online]. [viewed 2025-05-05]. Available from: https://www.shoplordmr.com/mr-products/mrf-140cg-magneto-rheological-fluid-1-liter

[20] *Material Manager for Altair Flux* [online]. [viewed 2025-05-05]. Available from: https://altairone.com/ Marketplace?tab=Info&app=Flux

[21] *Round Enamelled Copper Wire LioA EI/AIW* [online]. [viewed 2025-05-05]. Available from: https://hoangkhanh.net.vn/vi/san-pham/lioa-eiaiw-1

[22] SCHNEIDER, T., Y. HU, X. GAO, J. DUMAS, D. ZORIN and D. PANOZZO. A Large-Scale Comparison of Tetrahedral and Hexahedral Elements for Solving Elliptic PDEs with the Finite Element Method. *ACM Transactions on Graphics (TOG),* 2022*,* **41**(3), pp. 1-14. DOI 10.1145/3508372.

[23] TUAN, H.Q., T.M. HOANG, N.A. NGOC and O.T. LIM. Unveiling the Thermal Fingerprint of Magnetorheological Brakes: A Simulation Approach. In: *International Conference on Sustainability and Emerging Technologies for Smart Manufacturing*. Singapore: Springer, 2024, pp. 661-670. DOI 10.1007/978-981-97-7083-0_66.